Journal of Applied Polymer Science

Effect of Montmorillonite on the Rheological Properties of Dually Crosslinked Guar Gum-Based Hydrogels

Caterina Branca,[1] Cristina Crupi,[1] Giovanna D'Angelo,[1] Khaoula Khouzami,[1] Simona Rifici,[1] Annamaria Visco,[2] Ulderico Wanderlingh[1]

[1]Dipartimento di Fisica e Scienze della Terra, Università degli Studi di Messina, Messina, Italy

[2]Dipartimento di Ingegneria Elettronica, Chimica ed Ingegneria Industriale (DIECII), Università degli Studi di Messina, Messina, Italy

Correspondence to: C. Branca (E-mail: cbranca@unime.it)

ABSTRACT: One strategy to create chemical and physical cross-links simultaneously is to introduce into the chemical network hydrogen bonding with clay nanofillers. Understanding the relaxation mechanisms of these systems is crucially important and has drawn the extensive interest of many scientists. In this work, the influence of different amounts of montmorillonite on the structural and rheological properties of guar gum hydrogels was investigated. Depending on the clay content, different nanostructures were identified by X-ray diffraction (XRD) and their effect on the rheological properties of the dual hydrogels was studied. From stress and frequency sweep tests it emerged that all the samples exhibit a weak gel behavior and showed a maximum for G'' that can be ascribed to the breaking and reforming of transient physical crosslinks. This relaxation mode is more pronounced for the hydrogel for which a minimum in the swelling degree was observed. On the basis of these results, a model structure was proposed according to which the clay sheets act as effective multifunctional cross-linkers. The more homogeneously dispersed are the clay platelets, the higher is the density of physical crosslinks. © 2014 Wiley Periodicals, Inc. J. Appl. Polym. Sci. **2015**, *132*, 41373.

KEYWORDS: biomaterials; clay; crosslinking; rheology

Received 12 May 2014; accepted 2 August 2014

DOI: 10.1002/app.41373

INTRODUCTION

Hydrogels are three dimensional networks capable of absorbing large amounts of water while maintaining their dimensional stability.[1–3] The integrity in their swollen state can be maintained either by physical or chemical crosslinking. In chemically crosslinked hydrogels, the linear polymer chains are covalently bonded with each other via crosslinking agents. In contrast, physically crosslinked hydrogels are usually spontaneously formed by weak secondary forces such as hydrogen bonding, van der Waals interactions and ionic bonding.[4–7] Physical cross linked hydrogels have several advantages over chemical crosslinked hydrogels and also some disadvantages. The main advantage is the absence of potentially toxic crosslinking agents but this benefit must be weighed up against the weak mechanical properties these hydrogels offer. On the other side, for chemical hydrogels the mechanical and structural properties can be more easily tuned by adjusting the crosslinking concentration or by modifying the environmental conditions. In the last years, many efforts have been made to respond to a rising demand for new hydrogels with improved mechanical performance and new systems have been synthesized. Recently, dually crosslinked hydrogels, that is, hydrogels having chemical and transient-physical cross-links simultaneously[8–16] are receiving a great interest, since the intrinsic structure of these three-dimensional polymeric networks generates very interesting material properties. In these systems, breakable physical crosslinks may be introduced to the chemical network using hydrogen bonding with fillers,[17,18] ionic interactions between chains[19] or hydrophobic interactions.[15,20,21]

In this study we produced new guar gum-based hydrogels using glutaraldehyde as chemical crosslinker and montmorillonite as clay nanofiller. Clays are receiving intense research interest since they show unique properties even at very low filler volume fractions which can never be obtained by other nanofillers. They are extensively used in preparing polymer/clay nanocomposites with improved mechanical properties and thermal stability.[12,13,17,22–29]

Among them, biopolymer/clay nanocomposites attract significant interest because of their high biocompatibility, biodegradability, and accessibility.[30–37]

Guar gum (GG) is a natural hydrophylic, nonionic polysaccharide extracted from the endospermic seed of the plant Cyamopsis tetragonalobus. GG belongs to the large family of galactomannans and consists of a linear backbone of β (1→ 4)

-linked D-mannopyranose units with the presence of randomly attached α (1→ 6) -linked galactopyranose units as side chains.[38,39] Thanks to its high molecular weight and to the presence of extensive intermolecular entanglements by hydrogen bonding, GG can produce highly viscous solutions even at low concentration. Because of its low cost and easy availability, GG is widely applied in many industrial fields; it is commonly used as a thickening agent in cosmetics and in sauces, salad dressings and ice creams in the food industry.[40–43] In biological application, GG was used as a carrier for transdermal drug delivery system[44] and for colon targeted.[45] In fact, due to its nonionic nature, it is not affected by ionic strength or pH at moderate temperature so it can protect the drug in the stomach and small intestine environment.[46]

So far, many studies refer on the relaxation properties of GG hydrogels prepared by using separately chemical[47–49] or physical crosslinker[16,50] but, to our knowledge, there is no study about the effect of a clay on the relaxation mechanisms of guar gum-based hydrogels.

The aim of this work was to study the relation between the architecture of dually crosslinked hydrogels and their rheological properties. To this purpose, the dynamic viscoelastic properties of guar gum hydrogels with different montmorillonite (MMT) concentrations were measured over a wide range of stress amplitudes and then the linear viscoelastic behavior was investigated. The combined analysis of XRD, rheological, and swelling data allowed us to propose a model structure that can serve as a starting point for the proper design of high performing biocompatible hydrogels.

EXPERIMENTAL

Hydrogels Preparation

Commercially available guar gum, montmorillonite K10, and glutaraldehyde (GA) solution (Sigma Aldrich) were used. MMT is a hydrated alumina-silicate layered clay consisting of an edge-shared octahedral sheet of aluminum hydroxide between two silica tetrahedral layers.[51]

MMT employed in this study has a CEC of 70–100 meq/100 g. We used montmorillonite for its unique intercalation/exfoliation characteristics that can lead to platelets with very high stiffness and strength when dispersed in a polymer matrix.

Guar gum solutions were prepared by adding 0.8 g of guar gum to 50 mL of water; then they were magnetically stirred at 60°C for 24 h and left at room temperature for 24 additional hours for a complete dissolution. To protonate the hydroxyl groups of the polymer, a few drops of concentrated sulphuric acid were then added and the solutions were kept under magnetic stirring for 30 min. At the same time, different amounts of montmorillonite (0.008 g, 0.02 g, 0.04 g) were added to 50 mL of water and the mixtures were stirred for 24 h. Then, the montmorillonite solutions were carefully put in the guar gum solutions and all the mixtures were stirred for 4 h. Finally, an appropriate volume of 50% w/v of aqueous solution of GA was added to each solution corresponding to $r = 4.0$, where r represents the ratio between the cross-linker moles and the moles of repeating units of the polymer. The reaction mixtures were then stirred for 30 min and kept at room temperature.

After gelation was completed, the hydrogels were dialyzed using dialysis membranes with a cutoff 12,000–14,000 until the unreacted GA disappeared from the dialysis solvent. The presence of polymeric GA was detected at 235 nm and the monomeric GA at 280 nm.

According to the percentage of clay with respect to the polymer weight, we labeled the dually crosslinked hydrogels as 0, 1, 2.5, and 5% MMT.

Rheological Measurements

Dynamic rheometry is a powerful tool for monitoring the gelation (or cross-linking) and microstructural changes in a material through the examination of viscoelastic material functions, such as the storage and loss moduli, G' and G'', respectively.[52,53] The relative magnitudes of such dynamic shear moduli provide information regarding the proportion of the energy input that is stored elastically and that is dissipated during the flow over each cycle of frequency oscillation.

Rheological properties measurements were carried out by means of a rotational rheometer (Mod. SR5, Rheometric scientific) equipped with a sample environment controller. Experiments were performed with a 40 mm parallel plate geometry on cylindrical samples with a diameter of 40 mm and a height of 1 mm. The tests were carried out at room temperature (25°C). A dynamic stress sweep test was conducted on the material at a frequency of 1 Hz to determine its linear viscoelastic region (LVR). Frequency sweep tests were carried out in the frequency range 0.05–100 Hz at a constant stress (5 Pa) within the LVR and their viscoelastic parameters were measured. Each test was carried out in duplicate.

Swelling Measurements

Swelling studies were carried out by immersing the dried hydrogels in 50 mL of distilled water at 25°C. At regular intervals the hydrogel disks were removed from the medium and weighted after removing surface absorbed water with filter paper. Then the samples were immediately put back in the same swelling medium and kept soaking, until an equilibrium state of swelling was achieved. The water contents of the swollen hydrogels were calculated by using the following relation:

$$S(\%) = \frac{W_s - W_d}{W_d} \times 100 \quad (1)$$

W_S and W_d are the weights of the sample in the swollen and dry states, respectively. Each swelling experiment was repeated three times and the average values are reported.

X-ray Diffraction Analysis

X-ray diffraction measurements were performed at room temperature with a D8-ADVANCE Bruker diffractometer in Bragg-Brentano geometry using the Cu line $\lambda = 1.542$ Å. Each scan covered 2θ from 2° to 12° with a step size 0.02°, one second per step. During measurements, samples were held in a small chamber with 180° cylindrical Kapton windows. Measurements were performed on powder MMT and GG, and on dried dual hydrogels. For comparison, XRD patterns were also recorded

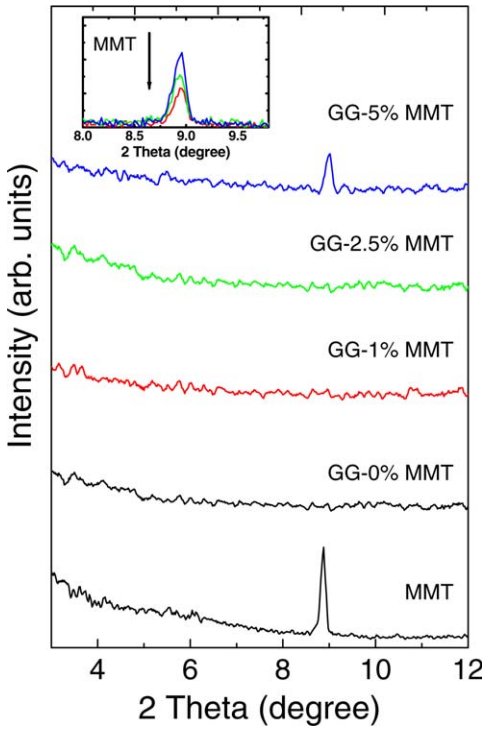

Figure 1. X-ray diffraction patterns of MMT and GG/MMT dual hydrogels in the dry state at different MMT concentrations. In the inset the XRD patterns of physical mixtures of guar gum and clay in the same amounts are reported. [Color figure can be viewed in the online issue, which is available at wileyonlinelibrary.com.]

for the dried physical mixtures (i.e., without crosslinker) at the same concentrations.

RESULTS AND DISCUSSION

X-ray diffraction is widely used to characterize the clay dispersion within a polymer matrix since it can provide evidence for the presence of different composites that can be obtained depending on the type and amount of nanoclay used: tactoids, intercalated, and exfoliated composites.[37,51,54] The results of the XRD analysis for the dual GG/MMT hydrogels are shown in Figure 1. The diffraction pattern of MMT shows a strong peak ($2\theta = 8.84°$) corresponding to a basal spacing of ≈10 Å. This diffraction peak is absent in the dual hydrogels with 1% and 2.5% MMT, indicating formation of an exfoliated structure homogeneously dispersed into the polymeric network. This results is in agreement with previous observations according to which immersion of low clay concentrations in low-ionic strength water solutions renders the clay fully dispersed into single sheets.[55] Further increasing the amount of MMT to 5%, gave a peak at the same 2θ value of MMT but lower than the pure clay. In order to verify if the absence of the diffraction peak can be attributed to a dilution effect rather than to exfoliation of the clay layers, the XRD patterns of the physical mixtures of guar gum and clay in the same amount were also recorded. As can be seen from the inset of Figure 1, in all these samples a diffraction peak is clearly visible thus confirming the exfoliation of the clay in the dual hydrogels. The position of the diffraction peak also indicates that no intercalation had occurred in the physical mixtures in agreement with previous results according to which polysaccharides with coiled or helicoidal structures, as is the case with guar gum, are only adsorbed in the external surface of clays.[32] From these observations, we hypothesized that at lowest concentrations investigated the clay layers are completely and uniformly dispersed or exfoliated in the polymer matrix, whereas for the hydrogel with 5% MMT the clay is present as microscale composite-tactoids.

Then we focused our attention on how these different types of nanostructures can affect the rheological behavior of the dual hydrogels. In Figure 2 the measured storage, G', and loss, G'', moduli are plotted as a function of the applied stress for the hydrogels with and without MMT. A linear viscoelastic (LVR) region is clearly observed for all the samples between 1 and 30 Pa and can be attributed to the existence of a balance between the rates of structural breakdown and rebuilding. Within this region, the G' values are always greater than the G'' values, indicating that the hydrogels show more elastic than viscous behavior. For higher stress values, a nonlinear behavior occurs, where G' decreases and G'' tends to increase first and then decreases. For all the samples a crossover point (also called critical stress σ_c) -the point at which the G' and G'' curves intersected-can be observed. At this point, the material collapses and the sample structure is irreversibly changed. By comparing the spectra for different MMT content, we can notice that the hydrogel with 2.5% of MMT offers the higher resistance against the imposed deformation since, for this system, we observe the higher σ_c value (≈440 Pa). The shift of the crossover point towards higher stresses indicates that hydrogel network is more stable at this MMT content.

Once the LVR range was defined, the "frequency sweep" test was performed. In Figure 3 the frequency dependence of G' and G'' for the prepared hydrogels is shown. As can be seen, the elastic modulus is always bigger than the viscous one for the entire frequency region investigated. However, our hydrogels cannot be considered ideal gels; in fact, in this case, G' should exhibit a pronounced plateau extending to times on the order of seconds and G'' should be significantly smaller than G′ in this region. Differently, in the investigated hydrogels, G' increases with frequency showing a restricted plateau around 2 rad/s whereas G'' shows a maximum around 0.25 rad/s and then decreases toward a minimum around 4 rad/s. At higher frequencies it increases again exhibiting a crossing point with G' around 50 rad/s.

The observed ω-dependence of both moduli witnesses the weak behavior of the prepared hydrogels. Furthermore, despite the similarity in the general trend, some differences can be observed in our samples depending on the clay concentration. In fact, increasing the MMT content up to 2.5% results in an increase of both moduli at whole frequency range investigated and, more interestingly, in a more pronounced increase in the G'' peak. A further adding of MMT results in a decrease of both moduli and in a flattening of this peak. The occurrence of a peak in the loss modulus was also observed for other systems such as PVA/borate[8,56] konjac/borax[57] and GG/borax[16,50,58] complex gels and it was considered indicative of the presence of

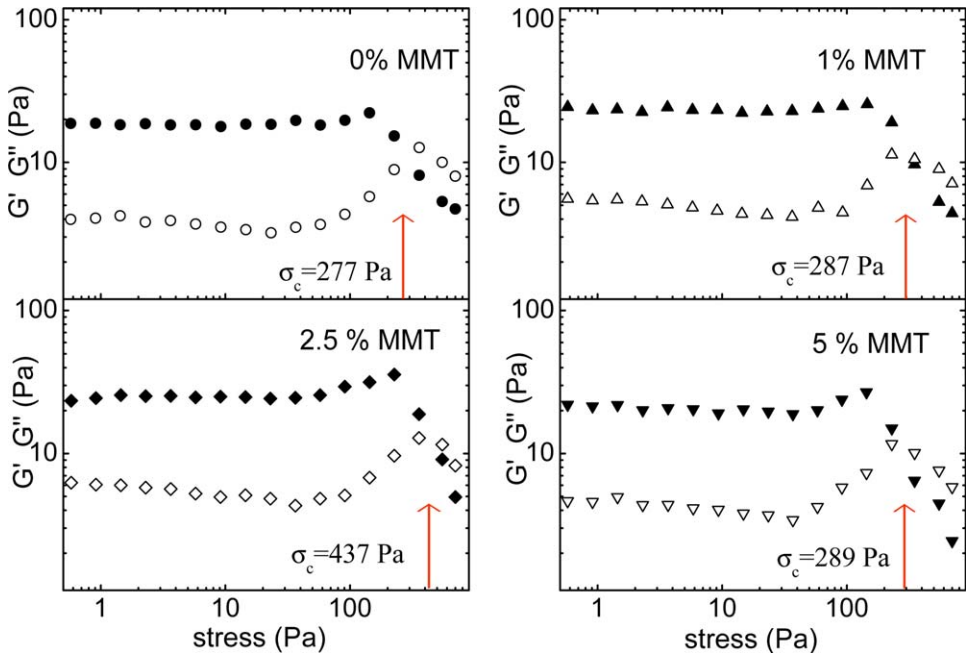

Figure 2. Elastic (full symbols) and viscous (open symbols) moduli versus oscillation stress for the GG/MMT hydrogels at different clay concentration in the stress sweep test. The arrows indicate the critical stress point σ_c. [Color figure can be viewed in the online issue, which is available at wileyonlinelibrary.com.]

transient crosslinks within the gels. As already stated, the presence of these breakable bonds is based on various noncovalent interactions that can coexist with the covalent ones in dual crosslink gels. This is the case of our systems chemically crosslinked by glutaraldehyde in presence of montmorillonite. In fact, the dispersion of MMT in water is favored by hydrogen bonding and dipole–dipole interactions between the water molecules and the clay surfaces. The hydrophilic nature of guar gum, besides inducing the helix-formation and the association of the helices, favors the absorption of the entangled chains over the hydrated clay surfaces: all of these factors (physical cross-links or entanglements) contribute to the formation of transient junction points that coexist with the permanent chemical crosslinks between the hydroxyl groups of GG and GA.

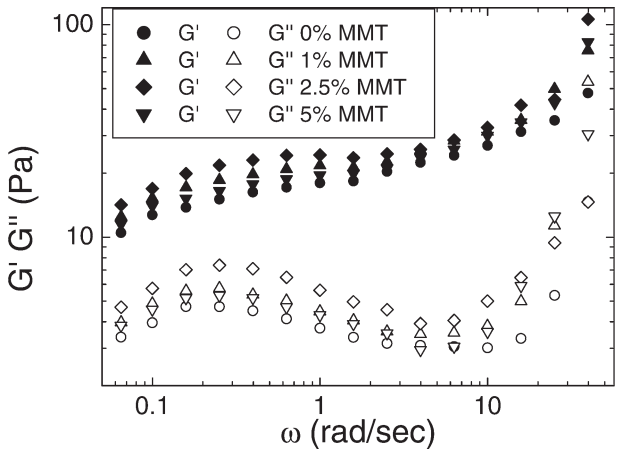

Figure 3. G' (closed symbols) and G'' (open symbols) as a function of angular frequency for the GG/MMT hydrogels at different MMT concentration.

Since our main interest was to evidence the effect of the physical crosslinks due to the presence of MMT, basing on the assumption that chemical and physical crosslinks can be described by a two-modes model,[8] we evaluated their individual contributions. To this purpose, the values of moduli G' and G'' for the hydrogel without MMT were subtracted from those of hydrogels prepared in presence of the clay. In such a way, we subtracted the effects of both chemical crosslinks and entanglements, this latter considered responsible for the broad but less pronounced peak in G'' observed for the hydrogel prepared without MMT. Since the polymer concentration is constant, any variation in the responsiveness of the system to frequency variations can now be only attributed to the presence of the clay. The result of this subtraction for the G' and G'' moduli is reported in Figure 4, where it emerges once more the occurrence of a dissipation process more evident for the hydrogel with a 2.5% MMT.

From these observations we can conclude that, in agreement with previous works,[8,16,50] the presence of the dissipation mode can be mainly ascribed to the breaking and reforming of transient physical crosslinks under stress conditions whose concentration is not merely proportional to the MMT concentration. In fact, in that case, contrary to what we found, we should expect a more pronounced relaxation process at the highest clay concentration investigated. Rather, we hypothesized a strict correlation between the overall architecture of the hydrogel and the underlying relaxation mechanisms. To unravel this aspect, we also investigated the swelling properties of the prepared hydrogels. In Figure 5 the swelling degree, $S(\%)$, for the investigated

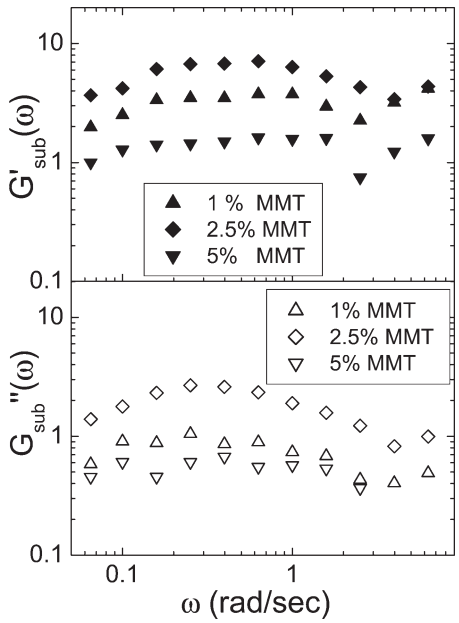

Figure 4. Dependence on the angular frequency of the contributions of the physical crosslinks to the elastic and viscous moduli, G_{sub}' and G_{sub}'', at different MMT concentrations (see text for details).

hydrogels is reported. As it can be seen, the swelling for all the samples occurs very fast in the first 3 min after which the swelling degree remains approximately constant. The incorporation of clay leads to a general decrease of the equilibrium swelling degree comparatively with the hydrogel prepared without MMT; more interestingly, it can be noticed that the hydrogel with 2.5% MMT exhibits the lower swelling capability. Considering that the different swelling capability of a hydrogel depends on the crosslink density, these results suggest the existence of a denser crosslink structure for the hydrogel with a 2.5% MMT.

Taking into account all these experimental evidences, we propose a simple structure model for the investigated hydrogels, schematically illustrated in Figure 6. We suppose that when low loads (1% and 2.5%) of MMT are added to the GG solution, the clay platelets over which the polymer is absorbed are homogeneously dispersed; the MMT platelets tend to bond together electrostatically, occupying the void space within the polymer network and thus creating a compact network. Consequently, up to a concentration of 2.5% MMT, the density of physical crosslinks increases thus justifying the observed enhancement in the dissipation mode. When an higher amount of MMT, is added, the hydrogel structure is significantly changed. In fact, according to the model proposed by Weiss et al.,[51] and in agreement with the reported XRD evidences, the clay layers are now aggregated in a "separated\micro-phase" inserted within the polymer matrix. As a consequence, a less dense, and less stable, crosslinked structure is formed. Moreover, because a smaller surface area is available for physical crosslinks, the observed flattening in the G'' peak at this concentration is justifiable.

This model accounts also for the same dependence on the clay content shown by the elastic modulus, the critical stress, σ_c, and the swelling degree. In fact, both G' and σ_c decrease in the order 2.5% > 1% > 5% > 0% MMT that is in the same order in which the swelling and hence the crosslink density, increases.

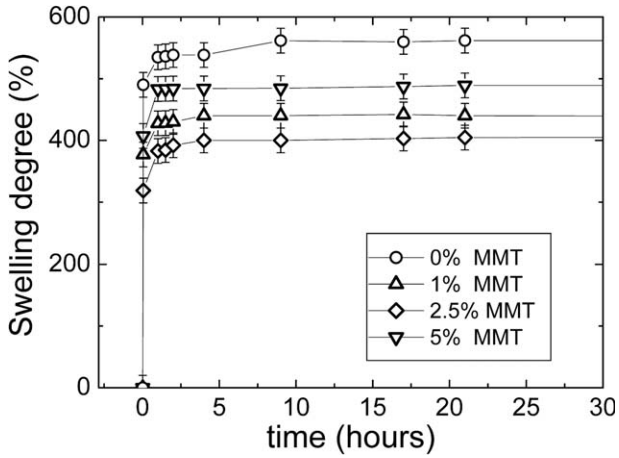

Figure 5. Swelling properties for the GG/MMT hydrogels at different clay content.

CONCLUSIONS

New guar gum-based hydrogels were prepared by incorporating montmorillonite into a polymeric matrix crosslinked by GA. The structure and dynamics of these hydrogels were investigated by XRD and dynamic rheology. We found that the concentration of clay play a critical role in controlling the structural and rheological properties. The diffraction patterns evidenced that the clay is exfoliated and homogenously dispersed inside the polymer matrix as the concentration increases up to 2.5%. At higher concentrations, aggregates are likely to be formed. Dynamic stress and frequency sweep tests evidenced that the presence of different composite nanostructures influences differently the rheological behavior of the investigated systems. From stress measurements we found that all the hydrogels show more elastic character than viscous one. A linear viscoelastic region is present for all the samples between 1 and 30 Pa, whereas for higher stress values a critical stress point σ_c can be observed. The highest σ_c value for the sample at 2.5% MMT suggests that at this clay concentration the hydrogel offers the higher resistance against the imposed deformation. From frequency sweep

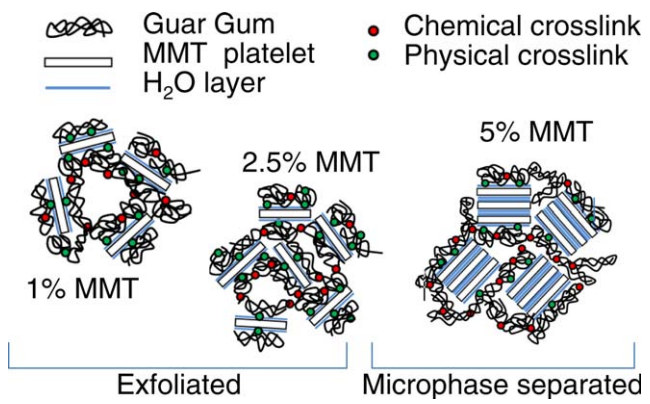

Figure 6. Schematic illustration of composite structures for the dual crosslinked GG/MMT hydrogels at different clay content. [Color figure can be viewed in the online issue, which is available at wileyonlinelibrary.com.]

tests it emerged that all the samples exhibit a weak gel behavior and show a broad peak for the loss modulus more pronounced for the hydrogel with 2.5% MMT. At this clay concentration, a minimum in the equilibrium swelling degree was also observed.

Starting from these experimental observations, we hypothesized for our systems the formation of a 3D structure in which reversible physical networks combine with the chemical network leading to a dual crosslink hydrogel. The presence of a more pronounced dissipation mechanism for the sample with 2.5% MMT can be ascribed mainly to the higher density of physical crosslinks between the polymer chains and the clay sheets over which they are absorbed. At this MMT concentration the filler effect of the clay is most pronounced inducing the formation of a denser crosslink network. At higher MMT content, it is reasonable hypothesize the presence of separated micro-phase aggregates inserted into the polymer matrix. The hampering effect tends to vanish since in this configuration fewer physical crosslinks are present. The strong relation between structural arrangements and mechanical behavior emerged also from the dependence on the MMT content of the elastic modulus, the critical stress point σ_c and the swelling degree. In fact, both G' and σ_c increase in the same order (MMT 0% < 5% < 1% < 2.5% MMT) in which the swelling decreases.

REFERENCES

1. Hoffman, A. S. *Adv. Drug Deliver. Rev.* **2002**, *54*, 3.
2. Kopecek, J.; Yang, J. *Polym. Int.* **2007**, *56*, 1078.
3. Peppas, N. A.; Hilt, J. Z.; Khademhosseini, A.; Langer, R. *Adv. Mater.* **2006**, *18*, 1345.
4. Chung, H. J.; Park, T.G. *Nano Today* **2009**, *4*, 429.
5. Jeong, B.; Kim, S. W.; Bae, Y. H. *Adv. Drug Deliver. Rev.* **2002**, *54*, 37.
6. Hennink, W. E.; Van Nostrum, C. F. *Adv. Drug Deliver Rev.* **2012**, *64*, 223.
7. Liu, Y.; Vrana, N.; McGuinness, G. *J. Biomed. Mater. Res. B* **2009**, *90B*, 492.
8. Narita, T.; Mayumi, K.; Ducouret, G.; Hebraud, P. *Macromolecules* **2013**, *46*, 4174.
9. Shibayama, M.; Takeuchi, T.; Nomura, S. *Macromolecules* **1994**, *27*, 5350.
10. Shibayama, M.; Uesaka, M.; Inamoto, S.; Mihara, H.; Nomura, S. *Macromolecules* **1996**, *29*, 885.
11. Rose, S.; Dizeux, A.; Narita, T.; Hourdet, D.; Marcellan, A. *Macromolecules* **2013**, *46*, 4095.
12. Gaharwar, A. K.; Sandhya, A. D.; Canter, J. M.; Wu, C. J.; Schmidt, G. *Biomacromolecules* **2011**, *12*, 1641.
13. Silioc, C.; Maleki, A.; Zhu, K.; Kjoniksen, A. L.; Nyström, B. *Biomacromolecules* **2007**, *8*, 1764.
14. Bocchinfuso, G.; Palleschi, A.; Mazzuca, C.; Coviello, T.; Alhaique, F.; Marletta, G. *J. Phys. Chem. B* **2008**, *112*, 6473.
15. Bocchinfuso, G.; Mazzuca, C.; Sandolo, C.; Margheritelli, S.; Alhaique, F.; Coviello, T.; Palleschi, A. *J. Phys. Chem. B* **2010**, *114*, 13059.
16. Mayumi, K.; Marcellan, A.; Ducouret, G.; Creton, C.; Narita, T. *ACS Macro Lett.* **2013**, *2*, 1065.
17. Haraguchi, K.; Takehisa, T. *Adv. Mater.* **2002**, *14*, 1120.
18. Lin, W. C.; Fan, W.; Marcellan, A.; Hourdet, D.; Creton, C. *Macromolecules* **2010**, *43*, 2554.
19. Henderson, K. J.; Zhou, T. C.; Ptim, K. J.; Shull, K. R. *Macromolecules* **2010**, *43*, 6193.
20. Miquelard-Garnier, G.; Demoures, S.; Creton, C.; Hourdet, D. *Macromolecules* **2006**, *39*, 8128.
21. Abdurrahmanoglu, S.; Can, V.; Okay, O. *Polymer* **2009**, *50*, 5449.
22. Tortora, M.; Gorrasi, G.; Vittoria, V.; Galli, G.; Ritrovati, S.; Chiellini, E. *Polymer* **2002**, *43*, 6147.
23. Gorrasi, G.; Tortora, M.; Vittoria, V.; Pollet, E.; Lepoittevin, B.; Alexandre, M. *Polymer* **2003**, *44*, 2271.
24. LeBaron, P. C.; Wang, Z.; Pinnavaia, T. J. *Appl. Clay Sci.* **1999**, *15*, 11.
25. Thostenson, E. T.; Li, C.; Chou, T. W. *Compos. Sci. Technol.* **2005**, *65*, 491.
26. Wang, J.; Lin, L.; Cheng, Q.; Jiang, L. *Angew. Chem. Int. Edit.* **2012**, *51*, 4676.
27. Wang, Q.; Mynar, J. L.; Yoshida, M.; Lee, E.; Lee, M.; Okuro, K.; Kinbara, K.; Aida, T. *Nature* **2010**, *463*, 339.
28. Shin, M. K.; Spinks, G. M.; Shin, S. R.; Kim, S. I.; Kim, S. J. *Adv. Mater.* **2009**, *21*, 1712.
29. Pinnavaia, T. J., Beall, G. W. Polymer-Clay Nanocomposites; Wiley: Chichester, West Sussex, U.K., **2000**.
30. Wang, S. F.; Shen, L.; Tong, Y. J.; Chen, L.; Phang, I. Y.; Lim, P. Q.; Liu, T. X. *Polym. Degrad. Stabil.* **2005**, *90*, 123.
31. Paluszkiewicz, C.; Stodolak, E.; Hasik, M.; Blazewicz, M. *FT-IR Spectrochim. Acta A* **2011**, *79*, 784.
32. Darder, M.; Colilla, M.; Ruiz-Hitzky, E. *Chem. Mater.* **2003**, *15*, 3774.
33. Zhang, Y.; Reddy Venugopal, J.; El-Turki, A.; Ramakrishna, S.; Su, B.; Lim, C. T. *Biomaterials* **2008**, *29*, 4314.
34. Abdollahi, M.; Rezaei, M.; Farzi, G. *J. Food Eng.* **2012**, *111*, 343.
35. Wang, X.; Du, Y.; Luo, J.; Lin, B.; Kennedy, J. F. *Carbohydr. Polym.* **2007**, *69*, 41.
36. Celis, R.; Adelino, M.A.; Hermosin, M. C.; Cornejo, J. *J. Hazard. Mater.* **2012**, *209-210*, 67.
37. Xu, Y.; Ren, X.; Hanna, M. A. *J. Appl. Polym. Sci.* **2006**, *99*, 1684.
38. McCleary, B. V.; Clark, A. H.; Dea, I. C. M.; Rees, D. A. *Carbohydr. Res.* **1985**, *139*, 237.
39. Petkowicz, C. L. O.; Reicher, F.; Mazeau, K. *Carbohyd. Polym.* **1998**, *37*, 25.
40. Rao M. S.; Kanatt, S. R.; Chawla, S. P.; Sharma, A. *Carbohydr. Polym.* **2010**, *82*, 1243.
41. Srivastava, M.; Kapoor, V. P. *Chem. Biodivers.* **2005**, *2*, 295.
42. Sostar-Turk, S.; Schneider, R. *Dyes Pigments* **1999**, *41*, 167.
43. Schneider, R.; Sostar-Turk, S. *Dyes Pigments* **2003**, *57*, 7.
44. Chourasia, M. K.; Jain, S. K. *Drug Deliv.* **2004**, *11*, 129.

45. Murthy, S. N.; Hiremath, S. R. R.; Paranjothy, K. L. K. *Int. J. Pharm.* **2004**, *272*, 11.

46. Rubinstein, A. *Drug Develop. Res.* **2000**, *50*, 435.

47. Barbucci, R.; Pasqui, D.; Favaloro, R.; Panariello, G. *Carbohydr. Res.* **2008**, *343*, 3058.

48. Sandolo, C.; Matricardi, P.; Alhaique, F.; Coviello, T. *Eur. Polym. J.* **2007**, *43*, 3355.

49. Cunha, P. L. R.; Castro, R. R.; Rocha, F. A. C.; de Paula, R. C. M.; Feitosa, J. P. A. *Int. J. Biol. Macromol.* **2005**, *37*, 99.

50. Coviello, T.; Matricardi, P.; Alhaique, F.; Farra, R.; Tesei, G.; Fiorentino, S.; Asaro, F.; Milcovich, G.; Grassi, M. *Express Polym. Lett.* **2013**, *7*, 733.

51. Weiss, J.; Takhistov, P.; McClements, D. J. *J. Food Sci.* **2006**, *71*, R107.

52. Pai, V.; Srinivasarao, M.; Khan, S. A. *Macromolecules* **2002**, *35*, 1699.

53. Mezger, T. G. *The Rheology Handbook*; Verlag: Hannover, Germany, **2002**.

54. Wang, B.; Yin, Y.; Liu, C.; Yu, S.; Chen, K. *J. Appl. Polym. Sci.* **2013**, *128*, 1304.

55. Ramsay, J. D. F.; Linder, P. J. *Chem. Soc., Faraday Trans.* **1993**, *89*, 4207.

56. Lin H.-L.; Yu, T. L.; Cheng, C-H. *Colloid Polym. Sci.* **2000**, *278*, 187.

57. Gao, S.; Guo, J.; Nishinari, K. *Carbohydr. Polym.* **2008**, *72*, 315.

58. Tayal, A.; Pai, V. B.; Khan, S. A. *Macromolecules* **1999**, *32*, 5567.